

Accepted Manuscript

Adiabatic plasma lens experiments at SPARC

J.B. Rosenzweig, F. Filippi, A. Zigler, M.P. Anania, G. Andonian, A. Biagioni, E. Chiadroni, A. Cianchi, A. Deng, M. Ferrario, G. Lawler, W. Lynn, N. Majernik, W. Mori, V. Shpakov



PII: S0168-9002(18)30166-9
DOI: <https://doi.org/10.1016/j.nima.2018.02.016>
Reference: NIMA 60545

To appear in: *Nuclear Inst. and Methods in Physics Research, A*

Received date: 20 November 2017
Revised date: 21 January 2018
Accepted date: 2 February 2018

Please cite this article as: J.B. Rosenzweig, F. Filippi, A. Zigler, M.P. Anania, G. Andonian, A. Biagioni, E. Chiadroni, A. Cianchi, A. Deng, M. Ferrario, G. Lawler, W. Lynn, N. Majernik, W. Mori, V. Shpakov, Adiabatic plasma lens experiments at SPARC, *Nuclear Inst. and Methods in Physics Research, A* (2018), <https://doi.org/10.1016/j.nima.2018.02.016>

This is a PDF file of an unedited manuscript that has been accepted for publication. As a service to our customers we are providing this early version of the manuscript. The manuscript will undergo copyediting, typesetting, and review of the resulting proof before it is published in its final form. Please note that during the production process errors may be discovered which could affect the content, and all legal disclaimers that apply to the journal pertain.

Adiabatic plasma lens experiments at SPARC

J.B. Rosenzweig¹, F. Filippi², A. Zigler³, M.P. Anania², G. Andonian¹, A. Biagioni², E. Chiadroni², A. Cianchi², A. Deng¹, M. Ferrario², G. Lawler¹, W. Lynn¹, N. Majernik¹, W. Mori¹, V. Shpakov²

¹*Dept. of Physics and Astronomy, University of California, Los Angeles, California 90095, USA*

²*Laboratori Nazionali di Frascati, INFN, Via E. Fermi, Frascati, Italia*

³*Hebrew University of Jerusalem, Jerusalem 91904, Israel*

Abstract

Passive plasma lenses in the underdense regime have been shown to give extremely strong linear focusing, with strength proportional to the local plasma ion density. This technique has been proposed as the basis of a scheme for future linear colliders that mitigates the Oide effect through adiabatic focusing. In this scenario the plasma density in the lens is ramped slowly on the scale of betatron motion, to funnel the beam to its final focus while forgiving chromatic aberrations. We present the physics design of an adiabatic plasma lens experiment to be performed at SPARC Lab. We illustrate the self-consistent plasma response and associated beam optics for symmetric beams in plasma, simulated by QuickPIC using exponentially rising density profiles. We discuss experimental plans including plasma source development and betatron-radiation-based beam diagnostics.

I. Introduction

Accelerators are flagship instruments that have enabled a large swath of scientific progress for most of the last century. In enabling high-energy colliding beam experiments, they have provided discovery potential up to the TeV energy scale [1], most recently yielding the first observation of the Higgs' boson [2]. They have also brought rapidly growing capabilities in imaging based on X-ray light sources, a field that in the last decade has produced the first X-ray laser, based on the free-electron laser (FEL) concept [3]. This innovation has opened the door to the resolution of atomic and molecular structure at the time (femtosecond and below) and length (Angstrom) scale, using the burgeoning techniques of coherent imaging [4].

The march of scientific progress permitted by accelerators is, however, threatened by the enormous costs associated with the enterprise: many X-ray FELs are currently under construction, with a price tag on the order of \$1B, while future colliders are presently estimated to cost over \$10B. This situation has been acknowledged in the particle physics community, with increasing urgency, for the last 30 years. As such, new acceleration paradigms have been demanded, based on new physical mechanisms and technologies, such as lasers, plasmas, and beam-driven wakefields.

Out of this effort, plasma-based acceleration schemes are emerging as an exciting new approach to creation of compact new accelerators. Due to plasmas already being in an ionized state, they overcome the problem of breakdown, and acceleration gradients of up to 50 GeV/m have been demonstrated, with TeV/m foreseen [5]. The development of a linear collider (LC) out of a new acceleration method is a long and scientifically challenging process, with many issues in fundamental beam physics that need to be resolved in a greater than decade-long program embraced by researchers worldwide.

One unique aspect of plasma accelerators is the existence of ultra-strong plasma-based transverse

45 focusing, which possesses unprecedented linear gradients. This strong, linear focusing is essential
 46 to the evasion of phase space dilution inside of the plasma accelerator *per se*. It is also highly
 47 flexible, with strength proportional to the plasma density as it varies along the beam propagation
 48 direction, $n_0(z)$. As such it may also be exploited in a unique way, to have a profound effect on
 49 LC design. This scenario is termed the *adiabatic plasma lens* [6], and it has been proposed to
 50 resolve a serious problem, the limit on final focusing schemes due to synchrotron radiation in the
 51 final focus elements, a phenomenon termed the Oide effect [7]. This innovative scheme permits
 52 “funneling” of beam to the LC interaction point, thus mitigating the effects of the radiation-
 53 induced chromatic aberrations.

54 In the PWFA blowout regime of the [8], where the beam density $n_b \gg n_0$, the beam channel is
 55 totally rarefied of plasma electrons. Under these conditions, the plasma response is very
 56 nonlinear, with relativistic electron velocities achieved, an amplitude-dependent period, and a
 57 large wave-breaking spike at the end of the first oscillation [9]. Inside of this electron-free
 58 “bubble”, beam electrons experience linear focusing fields arising from the pure ion column,
 59 with force $F_r = -2\pi e^2 n_0 r$. Note that for a commonly encountered plasma density near $n_0 \simeq$
 60 10^{17}cm^{-3} , that the linear force gradient is 900 TeV/m^2 , equivalent to a 3 MT/m magnetic
 61 gradient. As laboratory quadrupoles do not reach more than $\sim 600 \text{ T/m}$ in practice, this is four
 62 orders of magnitude beyond the current state of the art. Further, the pure EM acceleration in the
 63 plasma bubble is independent of r . Thus the e-beam transport and acceleration dynamics are
 64 similar to those of an RF linac with quadrupole focusing, a dramatic improvement over the linear
 65 PWFA. These traits have made the blowout regime a dominant scenario for development of the
 66 PWFA in the last 25 years.

67 The first studies of blowout regime plasma *focusing* was performed at the Argonne Wakefield
 68 Accelerator (AWA) facility [10], where equilibrium beam propagation was demonstrated with
 69 low brightness beams at low plasma density. This led to the initial observation of beam
 70 deceleration and acceleration, including use of witness beams, in the PWFA blowout regime [11].
 71 Later, short underdense ($n_b \gg n_0$) plasma lenses were first examined in a UCLA-FNAL
 72 experiment [12]. Notably, these measurements also showed focusing of strongly asymmetric
 73 (“flat”, as encountered in LCs) beams. Plasma focusing in the blowout regime has produced
 74 many novel effects, such as the collective beam refraction at a plasma boundary [13]. The
 75 experiments initiated at the AWA as well as subsequent investigations at SLAC FFTB [14],
 76 demonstrated long range guiding of beam in the underdense blowout regime [1,15] of the beam-
 77 plasma interaction.

78 II. Adiabatic plasma lens

79 Plasma focusing strength has led to the proposal to use the *underdense plasma lens* as an element
 80 of a linear collider final focus [16]; this is a strong advantage, as it permits very short focal
 81 length final focus lenses. Indeed, with the possibility of producing TeV beams in $\sim 100 \text{ m}$ plasma
 82 accelerators, the prospect of a km-scale final focusing system [17] is jarringly unpromising.
 83 Plasma lenses may potentially shrink the LC beam delivery system to the $<10\text{-metre}$ length scale.

84 As the strength of the plasma focusing gradient is proportional to $n_0(z)$ which may be easily
 85 tailored. The adiabatic plasma lens, takes advantage of this feature, relying on an adiabatic
 86 increase in focusing strength to funnel the beam size to very small spots. As the beam is in a
 87 slowly varying equilibrium in this scheme, one may strongly mitigate the chromatic aberrations
 88 introduced by the Oide effect.

89 The adiabatic plasma lens is a physical system in which the strength associated with the beam-
 90 plasma focusing interaction wake in the limit $n_b > n_0$, and where $k_p \sigma_z \gg 1$, where $k_p =$
 91 $\sqrt{4\pi r_e n_0}$ is the wavenumber of the plasma wake, i.e. $k_p = \frac{\omega_p}{c}$, and thus there is small
 92 longitudinal wake, ramps upward slowly in z . In this case the associated local betatron
 93 frequency k_β ramps upward in a similar manner, as one may write
 94 $k_\beta^2(z) = 2\pi r_e n_0(z)/\gamma = k_p^2(z)2/2\gamma$. Without ramping, one may define an equilibrium β -function,
 95 $\beta_{eq} = k_\beta^{-1}$. If the upward ramping of the plasma density is *adiabatic*, then β has a slowly changing
 96 quasi-equilibrium, simply written as $\beta_{q-eq}(z) \cong k_\beta^{-1}(z)$. The $n_0(z)$ profile defines a scale length,
 97 which should to preserve adiabaticity be much longer than the β -function, giving $L_s \equiv n_0(z)/n_0'(z)$
 98 $\gg \beta_{q-eq}(z)$. The increase in $n_0(z)$ serves to increase the beam density as well, as the spot area is simply
 99 $A(z) = 2\pi \varepsilon_n \beta_{q-eq}(z)/\gamma$. Thus n_b increases as $n_0^{1/2}$, and the underdense condition, $n_b/n_0 \square n_0^{-1/2} > 1$, is easiest
 100 to satisfy at the beginning of ramp. Indeed, the end of the ramp may be related to the limit $n_b/n_0 \sim 1$,
 101 as we shall see in simulations below. On the other hand, the starting point for the ramp is defined
 102 by the condition on the beam distribution that avoids a strong longitudinal wake response that
 103 has an onset when $k_p \sigma_z \sim 2$. Fortunately, during this phase of the interaction n_0 is low and the
 104 longitudinal wake is concomitantly weak.

105 For the requirements given above, a high brightness beam with significant peak current and low
 106 emittance is needed. At the SPARC Lab at INFN-LNF, such a system exists, as well as relevant
 107 plasma source technology, due to the current emphasis on plasma acceleration research at
 108 SPARC. Further, many relevant beam diagnostic systems are available that may be used to
 109 perform an adiabatic plasma lens experiment. To introduce the planned experiments, we begin
 110 by discussing PIC simulations of a likely scenario.

111 III. Simulations of Beam Dynamics

112 The beam plasma interaction and subsequent focusing is simulated by a particle-in-cell code,
 113 QuickPIC, which utilizes a frozen-plasma field scheme optimized to permit fast simulation of
 114 long interactions in plasma. The plasma density profile is taken to be exponentially rising over a
 115 six cm ramp, followed by a flat-top, as shown in Figure 1. The plasma density is initiated at a
 116 density of $n_0 = 5 \times 10^{15} \text{ cm}^{-3}$, and is increased by a factor of 400 to $n_0 = 2 \times 10^{18} \text{ cm}^{-3}$. The
 117 parameters for simulations of the beam-plasma interaction are given in Table 1, with beam
 118 parameters obtained from experimentally benchmarked simulations of the beam as produced,
 119 accelerated, and compressed, in the RF photoinjector at SPARC. The beam-plasma system
 120 initially obeys $k_p \sigma_z = 2$.

121 The initial and final beam spots are shown in Figure 2. The scaling of the beam density as $n_0^{1/2}$ is
 122 clearly displayed, with the line-out showing a factor of 20 times increase in beam density,
 123 validating the simple quasi-equilibrium model. In the final state at the flat-top, the ratio of the
 124 beam-to-plasma density is $n_b/n_0 = 1.15$, and blowout is just enforced. Nevertheless, the focusing is
 125 robust.

126 This is found not to be the case when then beam accesses the underdense regime, as is shown in
 127 Figure 3. The simulation of this case, where the same physical parameters are used as in Figure 2,
 128 with the exception of a pulse length longer by a factor of two (and thus a final beam density that
 129 would not exceed n_0) displays a radial oscillation of the plasma density at the end of the ramp,

130 indicative of the onset of a modulational instability. This is the type of instability that is
 131 employed by the AWAKE proton-driven PWFA [18] experiment, and is sought after in that case
 132 to resonantly excite longitudinal wakes through the introduction of a beam current structure
 133 periodic with λ_p . It can be seen that this occurs in the final stage of the adiabatic focusing process,
 134 and is clearly not a desirable effect for adiabatic plasma lens focusing.

135
 136

Table 1. Beam and plasma simulations for example adiabatic plasma lens experiment at SPARC.

Beam energy	110 MeV
RMS bunch length (σ_z)	75 μm
Normalized emittance ε_n	2 mm-mrad
Bunch charge	600 pC
Initial plasma density, n_0	$5 \times 10^{15} \text{ cm}^{-3}$
Initial matched β_{q-eq}	1.6 mm
Plasma scale length L_s	$\tau_l=1 \text{ cm}$
Total ramp length, L	6 cm

137

138 IV. Plasma Source

139 The type of plasma source needed for this experiment, an ablative capillary discharge, has been
 140 at use by UCLA for BNL ATF PWFA experiments, and also at SPARC, where it is employed in
 141 the PWFA program. The development and use of this discharge source was pioneered for
 142 accelerator and laser applications [19] at Hebrew Univ. This capillary discharge produces,
 143 confines, and shapes hydrogen-dominated plasmas. The nominal peak density of the plasma is
 144 tuned by the time delay between the discharge and the experimental application, *i.e.* the beam
 145 passage in our case. The plasma is formed by removal of material of the capillary walls, and is
 146 initiated by a laser pulse that ablates a small amount of surface near the cathode, where a voltage
 147 of a few tens of kV is applied. In the case, the capillary is made of plastic, and hydrogen is an
 148 abundant component of the plasma, a situation that can be reinforced by injection of hydrogen
 149 gas. This permits spectral analysis of hydrogen lines to obtain the plasma electron density and
 150 temperature [20], including the region interior to the capillary, which is optically accessible
 151 through the plastic. Initiated measurements at LNF have been performed on both standard and
 152 tapered capillaries, and are reported in a companion paper [21]. The tapering may be changed

153 simply by addition of new tapered transition regions (fabricated by 3D printing) having a variety
 154 of tapering angles and lengths. These shapes are pre-optimized by use of an analytical guide
 155 derived from previous measurements and analysis [22] that indicate the electron density should
 156 depend approximately on the radius of the capillary as $\sim R^{-3/2}$. The design is further informed by
 157 magneto-hydrodynamic code simulations. Preliminary measurements indicate that scale lengths
 158 of nearly a cm may be achieved with this approach.

159 V. Beam Diagnosis with Betatron Radiation

160 The oscillatory motion of an electron propagating under the influence of ion focusing in the
 161 blowout regime gives rise to *betatron radiation* [23,24,25,26]. This is a type of synchrotron or
 162 undulator radiation that has spectral characteristics that depend on the betatron amplitude of the
 163 electron in the ion-focusing channel. This amplitude dependence may permit determination,
 164 through a frequency spectrum measurement, of the beam emittance. This is because the
 165 undulator parameter is dependent on the betatron amplitude x_{00} as $K_u = k_\beta \gamma x_0$, where the
 166 betatron wavenumber $k_\beta = k_\beta / \sqrt{2\gamma}$.

167 If the oscillations are small $K_u \ll 1$, then one may easily relate this measurement to the
 168 emittance. In terms of normalized amplitude (single particle normalized phase space area ε_{n1}),
 169 one may write $K_u = \sqrt{k_\beta \varepsilon_{n1}}$. The amplitude dependence of K_u then produces a redshift in the
 170 wavelength of the on-axis undulator radiation, as $\lambda_r \cong (\lambda_\beta / 2\gamma^2) [1 + K_u^2 / 2]$, where $\lambda_\beta = \frac{2\pi}{k_\beta}$ is
 171 the betatron wavelength. Assuming a Gaussian phase space distribution, summation over
 172 amplitudes produces a simple expression for the rms normalized emittance in terms of the rms
 173 spectral width, as $\Delta\lambda_{rms} = 2\varepsilon_n / \gamma$. If $K_u \geq 0.5$, then the analysis is a bit more complex [27], but
 174 more information is available, in the form of radiation harmonics, as discussed below. When one
 175 measures this spectral width, the radiation emitted should be collected at constant γ . This requires
 176 a significant length of beam-plasma interaction where ion focusing is present while acceleration
 177 is not, which is the case in our final state (with the adiabatic ramp in density finished and flat $n_0(z)$
 178 is utilized), with the lensing condition $k_p \sigma_z > 2$.

179 For SPARC experiments, we analyze a scenario where the final plasma density is chosen to
 180 optimize this type of measurement, again choosing $n_0 = 1.5 \times 10^{18} \text{ cm}^{-3}$. In this case, even with
 181 a relatively small emittance of SPARC, the rms value of $K_u = 1.6$. With the betatron period of the
 182 fundamental photon wavelength is 12 nm (photon energy ~ 100 eV), and is thus in the EUV
 183 spectral range. The expected spectrum for this experiment has been simulated using the code
 184 SPECTRA, with the result given in that the spectrum has the expected fundamental energy, but
 185 with spectral spreading due to off-axis red shifting, the inherent spread in K_u due to the betatron
 186 amplitude distribution. This spectrum also shows evidence for harmonics up to $n=4$ due to the
 187 large K_u . It should be noted that the large K_u can be exploited to give enhanced information on
 188 the angles of the electron betatron trajectories in the plasma.

189 In implementing this revealing this measurement, we look to approaches used in previous
 190 experiments at both the BNL ATF in context of UCLA nonlinear inverse Compton scattering
 191 (ICS) experiments [28,29] and at LBNL BELLA laser plasma accelerator betatron radiation
 192 experiments [26]. As these previous measurements were in different spectral region, we must
 193 change the dispersive element in the spectrometer, while keeping much of the method intact. The
 194 system for ICS measurements at the ATF gives a single shot, double differential spectral (DDS)

195 measurement in the 5-25 keV range, employing a bent, multi-layer, Si-Mo crystal for dispersing
196 the spectrum. The bent multi-layer disperses the wavelengths in the crystal bend plane, while
197 leaving the angular information in the vertical direction (along that of a collimating slit) of the
198 image at the micro-channel plate detector.

199 The spectrum of nonlinear ICS is quite similar to that of the betatron radiation, as both are
200 effectively large K_u undulators with a systematic variation in strength. In Ref. 45, an analysis of
201 near-axis radiation collected in this spectrometer is given and is in analogy to the betatron
202 amplitude analysis described above, yielding information about the beam-laser interaction.

203 The geometry employed in the BNL ICS experiments will be merged with that used in the
204 BELLA betatron radiation measurements, with a collimating slit introduced. In this case we will
205 substitute the bent multi-layer crystal with an EUV capable grating [30]. This system can utilize
206 an MCP employed at UCLA EUV ICS experiments [31]. As an alternative approach, one may
207 consider employing a CCD array as was used in single-photon-per-pixel mode to give the soft-X-
208 ray spectrum in BELLA measurement system.

209 VI. Conclusions

210 The rationale and physics goals underpinning the adiabatic plasma lens experiment at the
211 SPARC Lab has been presented. A robust scenario for testing the concepts involved, in which
212 the beam is adiabatically focused to a density 20 times that of the initial value is outlined, with
213 the aid of scaling laws and detailed PIC simulations. The major consequences of failing to obey
214 the blowout conditions on the adiabatic plasma lens performance are identified.

215 We have reviewed briefly the progress made on developing adequate plasma source for this
216 experiment based on existing discharge-based approaches but with tailored entrance boundaries
217 to control the hydrodynamic expansion of the gas and the expansion dynamics plasma after
218 formation. The details of such experimental development are discussed in Ref. 20. The physics
219 that can be revealed through betatron radiation spectral measurements have been analyzed, and a
220 spectrometer system designed to obtain the relevant experimental signals has been identified.

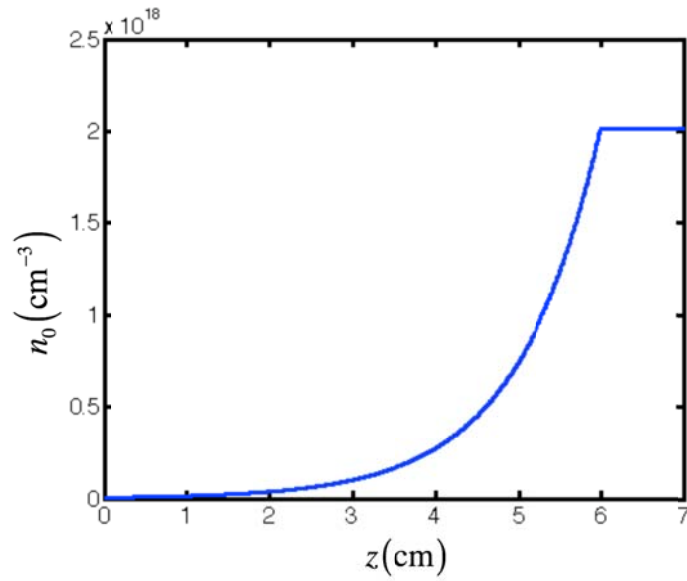
221 With the initiation of the experimental program on plasma acceleration and lensing at SPARC
222 now underway, the adiabatic plasma lens measurements may begin within the next year. This
223 experiment should provide an invaluable demonstration of the unique utility of plasma lensing in
224 the context of advanced collider physics applications. In this regard, future work in simulations
225 and experiments will concentrate on the focusing of asymmetric (transversely elliptic-shaped)
226 beams, due to their complex beam-plasma interaction physics and the high relevance to collider
227 scenarios.

228 Acknowledgments

229 This work supported by the U.S. DOE contract DE-SC0009914, and US Dept. of Homeland
230 Security Grant 2014-DN-077-ARI084-01.

231

232

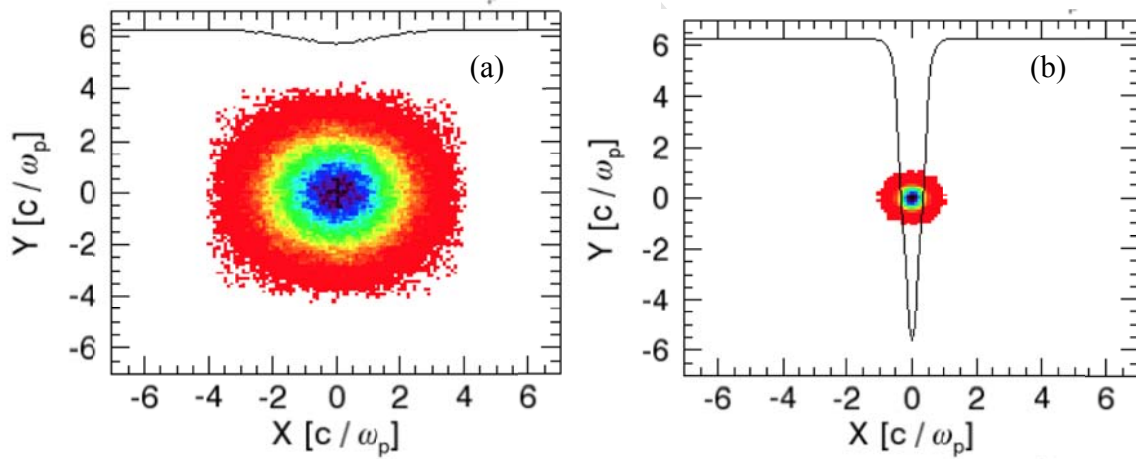


233

234

Figure 1. Plasma density profile used in adiabatic lens simulations.

235



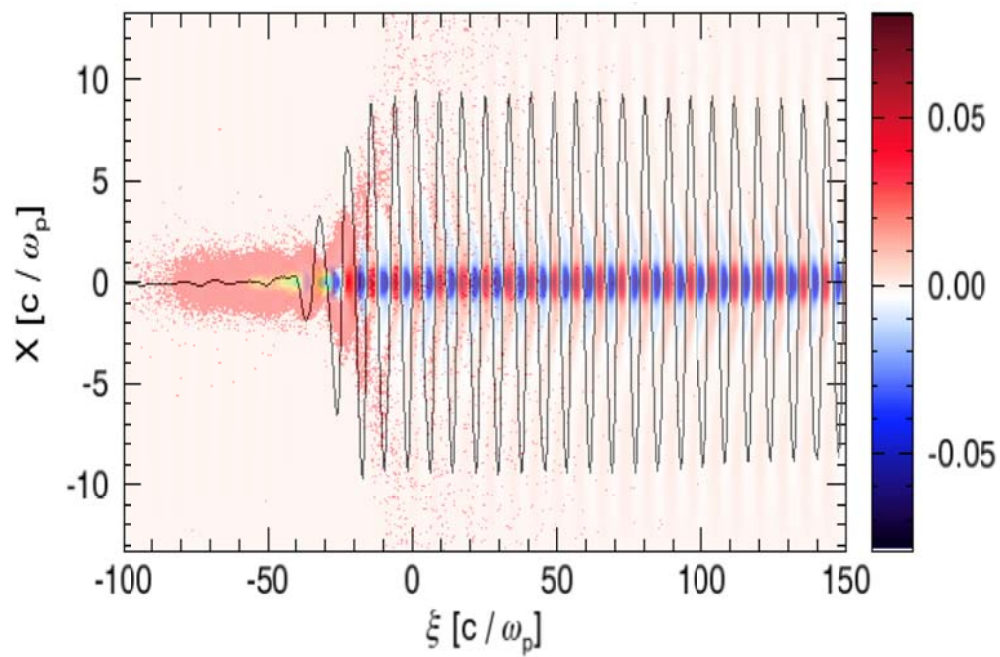
236

237

238

Figure 2(a) Initial and (b) final beam x - y distributions from PIC simulation of adiabatic plasma lens with parameters as described in Table 1, shown in linear red-blue color map and line-out.

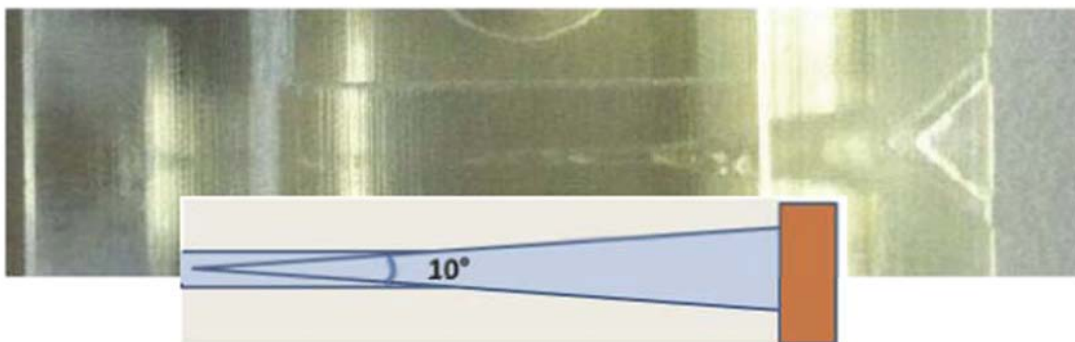
239



240

241 **Figure 3. Final beam x - ξ distributions from PIC simulation of adiabatic plasma lens with same parameters as in Figure 2,**
 242 **but with double the bunch length, i.e. $\sigma_z=150 \mu\text{m}$. Also shown, longitudinal wakefield on-axis profile.**

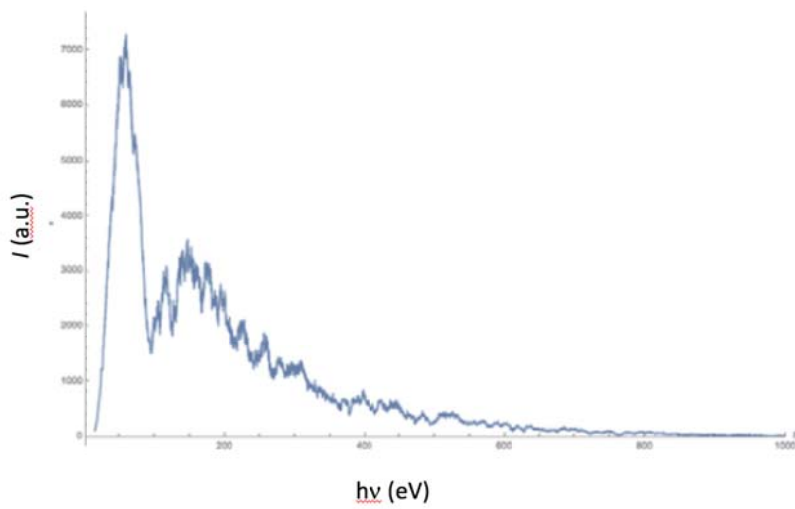
243



244

245 **Figure 4. Photograph of the tapered plastic capillary for production of ramped plasma density profile needed for**
 246 **adiabatic lens experiments, with schematic of the tapering scheme.**

247



248

249

Figure 5. SPECTRA calculation of spectral content of betatron radiation for example experimental scenario.

250

251 **References**

1. I. Blumenfeld et al., *Nature* **445**, 741 (2007)
2. S. Chatrchyan, et al., *Physics Letters B* **716**, 30 (2012)
3. C. Pellegrini, *Eur. Phys. J. H* **37**, 659-708 (2012)
4. T. Ekeberg, et al. *Phys. Rev. Lett.* **114**, 098102 (2015)
5. J.B. Rosenzweig, et al., *Nucl. Instr. and Methods A* doi:10.1016/j.nima.2011.01.073 (2011).
6. P. Chen, K. Oide, A.M. Sessler and S.S. Yu, *Phys. Rev. Lett.* **64**, 1232 (1990)
7. K. Oide. *Phys. Rev. Lett.* **61**, 1713 (1988)
8. J. B. Rosenzweig, et al., *Phys. Rev. A -- Rapid Comm.* **44**, R6189 (1991).
9. J. B. Rosenzweig, N. Barov, M. C. Thompson, and R. B. Yoder *Phys. Rev. ST Accel. Beams* **7**, 061302 (2004); N. Barov, J. B. Rosenzweig, M. C. Thompson, and R. B. Yoder, *Phys. Rev. ST Accel. Beams* **7**, 061301 (2004)
10. N. Barov, M.E. Conde, W. Gai, and J.B. Rosenzweig, *Physical Review Letters.* **80**, 81 (1998)
11. N. Barov, et al., *Phys. Rev. ST Accel. Beams* **3** 011301 (2000).
12. M. C. Thompson, et al., *Phys. Plasmas*, **17**, 073105 (2010)
13. P. Muggli, et al., *Phys. Rev. ST Accel. Beams* **4** (2001)
14. C.E. Clayton, et al., *Phys. Rev. Lett.* **88**, 154801 (2002)
15. M. Hogan, et al. *Phys. Rev. Lett.*, **95**, 054802 (2005)
16. P. Chen, S. Rajagopalan, and J. Rosenzweig, *Phys. Rev. D* **40**, 923 (1989).
17. P. Raimondi and A. Seryi, *Phys. Rev. Lett.* **86**, 3779 (2001)
18. A. Caldwell, K. Lotov, A. Pukhov, F. Simon, *Nature Physics* **5**, 363–367 (2009)
19. Y. Ehrlich, C. Cohen, A. Zigler, J. Krall, P. Sprangle, E. Esarey, *Phys. Rev. Lett.* **77** (1996)
20. H. R. Griem, *Plasma spectroscopy* McGraw-Hill, 1964.
21. F. Filippi, et al., these proceedings.
22. D. Kaganovich et al., *Appl. Phys. Lett.* **71**, 2925 (1997).
23. S. Kneip, et al. *Phys. Rev. Lett.* **100**, 105006 (2008)
24. Kim Ta Phuoc, et al., *Phys. Rev. Lett.* **97**, 225002 (2006)
25. S. Corde, et al., *Phys. Rev. Lett.* **107**, 255003 (2011)
26. Aihua Deng, et al., *Phys. Rev. ST Accel. Beams* **15**, 081303 (2012)
27. G.R. Plateau, et al., *PRL* **109**, 064802 (2012)
28. Y. Sakai, et al., *Phys. Rev. ST Accel. Beams*, **18**, 060702 (2015)
29. Y. Sakai et al., *Phys. Rev. ST Accel. Beams*, **20**, 060701 (2017)
30. D.L. Voronov, et al. *Journal of Physics: Conference Series* **425** (2013) 152006
31. G. A. Krafft, A. Doyuran, and *Phys. Rev. E* **72**, 056502 (2005)

Highlights

- Passive plasma lenses can, by virtue of their extraordinary, locally tunable strength, can be used in a new type of focusing, where electron beams are adiabatically diminished in transverse size.
- This adiabatic plasma lens may provide an essential method for avoiding the Oide limit on focusing in TeV-class linear colliders.
- A first experimental test of adiabatic lensing is proposed to take place at the SPARC Lab at INFN-LNF in Frascati, Italy. Detailed simulations illustrate the feasibility of this experiment.
- Development of the unique ramped-density plasma source at INFN-LNF for this experiment is reported.
- Diagnosis of the beam focusing to few micron size by using betatron radiation is described.